Asian Journal of Pharmaceutical Sciences 16 (2021) 643–652

Available online at www.sciencedirect.com

ScienceDirect

journal homepage: www.elsevier.com/locate/AJPS

Original Research Paper

Investigating the crucial roles of aliphatic tails in disulfide bond-linked docetaxel prodrug nanoassemblies

Yuequan Wang[1], *Cong Luo*[1], *Shuang Zhou, Xinhui Wang, Xuanbo Zhang, Shumeng Li, Shenwu Zhang, Shuo Wang, Bingjun Sun, Zhonggui He, Jin Sun*[*]

Shenyang Pharmaceutical University, Shenyang 110016, China

ARTICLE INFO

Article history:
Received 25 December 2020
Revised 21 January 2021
Accepted 12 February 2021
Available online 25 February 2021

Keywords:
Docetaxel
Aliphatic prodrug
Disulfide bond
Self-assembly capacity
In vivo drug delivery fate

ABSTRACT

Disulfide bond-bridging strategy has been extensively utilized to construct tumor specificity-responsive aliphatic prodrug nanoparticles (PNPs) for precise cancer therapy. Yet, there is no research shedding light on the impacts of the saturation and cis-trans configuration of aliphatic tails on the self-assembly capacity of disulfide bond-linked prodrugs and the *in vivo* delivery fate of PNPs. Herein, five disulfide bond-linked docetaxel-fatty acid prodrugs are designed and synthesized by using stearic acid, elaidic acid, oleic acid, linoleic acid and linolenic acid as the aliphatic tails, respectively. Interestingly, the cis-trans configuration of aliphatic tails significantly influences the self-assembly features of prodrugs, and elaidic acid-linked prodrug with a trans double bond show poor self-assembly capacity. Although the aliphatic tails have almost no effect on the redox-sensitive drug release and cytotoxicity, different aliphatic tails significantly influence the chemical stability of prodrugs and the colloidal stability of PNPs, thus affecting the *in vivo* pharmacokinetics, biodistribution and antitumor efficacy of PNPs. Our findings illustrate how aliphatic tails affect the assembly characteristic of disulfide bond-linked aliphatic prodrugs and the *in vivo* delivery fate of PNPs, and thus provide theoretical basis for future development of disulfide bond-bridged aliphatic prodrugs.

© 2021 Shenyang Pharmaceutical University. Published by Elsevier B.V.
This is an open access article under the CC BY-NC-ND license
(http://creativecommons.org/licenses/by-nc-nd/4.0/)

1. Introduction

Despite great progression in diagnosis techniques and therapeutic methods, malignant tumor is still a serious threat to human [1]. Over the past years, multiple treatments such as surgical removal, chemotherapy, radiotherapy and immunotherapy have been widely applied for cancer therapy [2]. Among them, systemic chemotherapy holds a significant position in clinics due to its wide applicability and the broad-spectrum antitumor effects, especially for the patients with widespread metastatic focuses [3]. However,

* Corresponding author.
E-mail address: sunjin@syphu.edu.cn (J. Sun).
[1] These authors contributed equally to this work.
Peer review under responsibility of Shenyang Pharmaceutical University.

https://doi.org/10.1016/j.ajps.2021.02.001
1818-0876/© 2021 Shenyang Pharmaceutical University. Published by Elsevier B.V. This is an open access article under the CC BY-NC-ND license (http://creativecommons.org/licenses/by-nc-nd/4.0/)

the clinical outcomes of most chemotherapeutic drugs are far from satisfactory due to various disadvantages, such as poor physicochemical properties, rapid blood clearance, insufficient tumor accumulation and severe systemic toxicity, which result in low therapeutic efficacy and high toxicity risks [4]. For instance, docetaxel (DTX) is a very hydrophobic compound with broad anticancer spectrum [5]. But the oral absorption efficiency of DTX is extremely low, resulting in poor oral bioavailability. Formulating DTX into injectable dosage form has been the only choice for its clinical application [5,6]. However, it's challenging to dissolve the hydrophobic molecule in aqueous solution. As a result, large amount of Tween 80 and ethanol were utilized to solubilize DTX in the commercially available injections, resulting in excipient-related severe side effects. More importantly, DTX injection could be quickly metabolized following intravenous administration, resulting in low tumor accumulation and poor antitumor activity [7]. Therefore, drug delivery systems with high efficiency and security has always been desired for clinical chemotherapy [8,9].

Nano-drug delivery systems (NDDS) held a bright future for efficient cancer therapy, owing to many obvious advantages in extending the circulation time in blood and enhancing the drug accumulation at tumor site via the enhanced permeability and retention (EPR) effect [10-16]. Several nanomedicines have been used in clinical tumor treatment, such as DOXIL® and Abraxane® [17]. Even so, most conventional NDDS have long been criticized for unsatisfactory clinical translation, due largely to complex preparation process, low drug loading rate, and potential biosafety risks of carrier materials [18]. In recent years, self-assembled carrier material-free NDDS have been developed as promising nanoplatforms to improve drug delivery efficiency [19]. Certain drugs or prodrugs were found to self-assemble into uniform nanoassemblies without the help of any amphipathic materials, thus significantly simplifying the fabrication process and improving drug loading efficiency [20]. Particularly, prodrug strategy has been proven to improve the physicochemical properties and to mitigate toxicity of chemotherapeutic agents [21]. Several chemotherapeutic prodrugs have been developed and entered clinical trials, such as elaidic acid-cytarabine prodrug, docosahexaenoic acid-paclitaxel prodrug, and elaidic acid-gemcitabine prodrug [22]. Disappointingly, the clinical outcomes of these prodrugs were far from satisfaction, probably due to the rapid clearance of these small-molecule prodrugs from the body. Additionally, parent drugs with pharmacological activity could not be easily released from the highly hydrophobic prodrugs, such as ester bond-linked docosahexaenoic acid-paclitaxel prodrug, which has been found to be one of the main dominant reasons for its clinical trial failure [23,24]. Therefore, it's necessary to develop tumor stimuli-responsive prodrug-based NDDS to combine the advantages of conjugation chemistry and NDDS [25].

Tumor cells are characterized as a reductive intracellular microenvironment with rising intracellular glutathione (GSH) level compared with normal cells [26,27]. The reduction gradient has been widely used to design reduction-responsive NDDS [28,29]. Our group has previously developed a series of lipophilic prodrug-based nanoassemblies of taxanes for efficient cancer chemotherapy [30-33]. Several redox-sensitive prodrugs were synthesized by conjugating taxanes with lipophilic moieties via single thioether bond, disulfide bond or dithioether bond [34-36]. Disulfide bond-linked PNPs not only showed redox hypersensitization, but also played important role in the self-assembly capacity of lipophilic prodrugs [37]. Moreover, the location of the disulfide bond in the chemical linker chains was found to have important effects on the redox sensitiveness of aliphatic PNPs [38]. On the basis of these previous investigations, we further supposed that different aliphatic chains with various saturation and cis-trans configuration might also affect the self-assembly characteristic, redox sensitiveness and *in vivo* drug delivery fate of disulfide bond-coupled lipophilic PNPs.

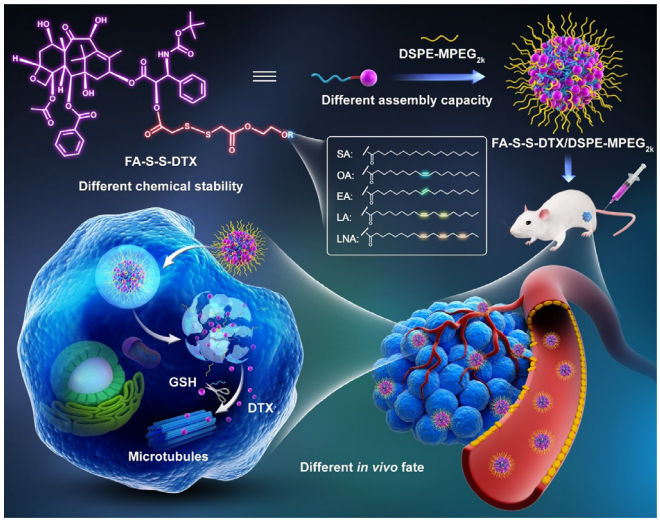

Scheme 1 – The disulfide bond–linked PNPs by using different fatty acids with different saturation and cis-trans configuration as aliphatic tails for cancer therapy.

To test our hypothesis, five fatty acids (FAs) were utilized to synthesize disulfide bond-bridged prodrugs of DTX (FA-S-S-DTX), including stearic acid (SA, a saturated FA), oleic acid (OA, a monounsaturated cis-FA), elaidic acid (EA, a monounsaturated trans-FA), linoleic acid (LA, a polyunsaturated cis-FA) and linolenic acid (LNA, a polyunsaturated cis-FA). The five prodrugs were abbreviated as SA-S-S-DTX, EA-S-S-DTX, OA-S-S-DTX, LA-S-S-DTX, and LNA-S-S-DTX, respectively (Scheme 1). The impacts of the aliphatic tails on the chemical stability of prodrugs and the self-assembly capacity and *in vivo* delivery fate of PNPs were comparatively probed in detail.

2. Experimental section

2.1. Materials

DTX and DiR were sourced from Dalian Meilun Biotechnology Co., Ltd (Dalian, China). 1-hydroxybenzotriazole (HOBt), 1-(3-Dimethylaminopropyl)−3-ethylcarbodiimide hydrochloride (EDCI) and 4-dimethylaminopyrideine (DMAP) were sourced from Energy Chemical (Shanghai, China). Dithiodiglycolic

acid was bought from TCL(Shanghai) Development Co., Ltd (Shanghai, China). SA, OA, EA, LA, LNA and coumarin-6 (C-6) were obtained from Aladdin (Shanghai, China). Dithiothreitol (DTT), cell culture media and MTT were bought from Beijing Solarbio Science & Technology Co., Ltd. (Beijing, China). DSPE-MPEG$_{2000}$ was bought from A. V. T. (Shanghai, China) Pharmaceutical Technology Co., Ltd (Shanghai, China). Cell culture dishes and plates were bought from NEST Biotechnology Co., Ltd (Wuxi, China).

2.2. Synthesis of prodrugs

Five prodrugs (SA-S-S-DTX, EA-S-S-DTX, OA-S-S-DTX, LA-S-S-DTX, LNA-S-S-DTX) were provided and optimized by Suzhou Yutai Pharmaceutical Technology Co. LTD. Specifically, the solution of toluene for FAs (SA, EA, OA, LA or LNA, 10 mmol) was added to 30.9 ml ethylene glycol (0.13 mol). With P-toluenesulfonic acid as catalyst, the mixture was stirred for 2 h at 110 °C. Then, methylbenzene layer was collected, and ethylene glycol layer was extracted with methylbenzene, and the two were mixed. Finally, oily liquid (fatty acid 2-hydroxyethyl ester) was extracted *via* column chromatography with a yield of 58.6%. Thereafter, the oily liquid (0.83 mmol) and 2,2′-di-thiodiglycolic acid anhydride (1.25 mmol) were added into dichloromethane, and DMAP was instilled slowly. Finally, the above intermediate product, DMAP, EDCI and HOBt were mixed in dichloromethane and stirred at 0 °C for 1 h. Then, the DTX was instilled to the reaction and sequentially stirred for 48 h at 25 °C in protective nitrogen. The prodrugs were purified by chromatography (100% acetonitrile) with a yield of 62.1%.

2.3. Preparation of PEGylated PNPs and dtx solution

Briefly, prodrugs (1 mg) were dissolved in anhydrous ethanol. And the ethanol solution was dropwise added into water (2 ml) under magnetic stirring. The ethanol was evaporated and obtained 0.5 mg/ml of non-PEGylated PNPs. Besides, PEGylated PNPs were prepared. Prodrugs and DSPE-MPEG$_{2000}$ were dissolved in anhydrous ethanol. Under magnetic stirring, the mixture was instilled into water. The ethanol was evaporated at 32 °C water bath and obtained 2 mg/ml of PNPs. Besides, C-6 or DiR was encapsulate into prodrugs nanoparticles (NPs) by dropwise adding the mixed ethanol solutions of prodrug, DSPE-MPEG$_{2000}$ and dye into deionized water to prepared dye-labeled PNPs. The ethanol was evaporated under vacuum at 32 °C water bath. The size and zeta potential of PNPs were determined. By staining with phosphotungstic acid, the microstructure of PNPs was detected by transmission electron microscope. The DTX solution (DTX sol) was prepared in the laboratory according to the commercial DTX injections (TAXOTERE®) formula. Briefly, 20 mg DTX was dissolved in 0.5 ml Tween 80, and 1.5 ml aqueous solution of 95% ethanol (13%, w/w) was added. Then the above solution was diluted to 1 mg/ml with saline before use.

2.4. Stability of PNPs

The chemical stability of prodrugs was investigated by determination of purity using High Performance Liquid Chromatography (HPLC, HITACHI, JAPAN). The prodrugs (purity >98%) were stored in a dark and dry place at −20 °C. Samples were taken and dissolved in acetonitrile (1 mg/ml) to determine at timed intervals by using HPLC. The colloidal stability of PEGylated PNPs was studied using particle size variation as the criterion. PEGylated NPs were stored in a 4 °C environment for two months. Samples were taken to determine at timed intervals by using Malvern Zetasizer.

2.5. Drug release from PNPs

To investigate the DTX release profiles under reductive environment, PNPs were incubated in PBS containing 30% ethanol with DTT at 37 °C. At the set time points, the DTX concentrations in the release medium were measured by HPLC.

2.6. Cell culture

Mouse breast tumor cells line (4T1 cells), mouse hepatoma tumor cell (Hepa1-6 cells) and human normal liver cells (L02 cells) were obtained from the cell bank of Chinese Academy of Sciences (Beijing, China). The Hepa1-6 cells were cultured with DMEM medium containing fetal bovine serum (FBS), streptomycin and penicillin. The 4T1 and L02 cells were cultured in RPMI 1640 medium with FBS, streptomycin (100 μg/ml) and penicillin (100 units/ml). All cells were maintained in a humidified cell incubator.

2.7. Cytotoxicity assays

The *in vitro* antiproliferative activity of DTX sol and PNPs against 4T1, Hepa1-6 and L02 cell lines were explored by MTT viability assay. Briefly, cells were seeded into 96-well plates (2000 cells/well) and were incubated in a humidified cell incubator until the cells stick to the wall. Then nutrient-free medium was discarded and fresh medium with DTX sol or PNPs were added. The cells were further incubated for 48 h or 72 h. Then, 25 μl of MTT solution was added to incubated for another 4 h. After 4 h cultivation, the MTT-contained medium was discarded, then dimethyl sulfoxide (DMSO) was utilized (200 μl/wells) to dissolve the formed formazan crystals. After a 10 min shake, the absorbance was detected by microplate reader (490 nm).

2.8. Intracellular DTX release

To test the DTX release from PNPs, 4T1 cells were put into 24-well plates (1×10^5 cells/well). Then the fresh medium contained with PNPs (DTX equivalent concentrations: 100 or 500 ng/ml) were added and incubated for 48 h. Then the cells were broken by ultrasonic crushing method and mixed well with the culture medium. Using diazepam as internal standard, the released DTX was determined by UPLC-MS-MS (Waters Co., Ltd.).

2.9. Cellular uptake

4T1 cells were put into 24-well cell-culture plate loaded with circle microscope cover glass (1×10^5 cells/ well)

and cultivated for 24 h to evaluate the cellular uptake of PNPs. Then the old medium was replaced with new medium containing C-6 or C-6-labled PNPs with equivalent C-6 concentration of 250 ng/ml for 2 h, respectively. The extracellular drug was washed, and the cells were fixed by 4% paraformaldehyde and the nuclei were counterstained by Hoechst33342. The cells-attached circle microscope cover glasses were photographed utilizing a confocal laser scanning microscope (CLSM). Besides, 4T1 cells were seeded into cell culture plate for 12 h, and then cells were treated with C-6 solutions, C-6-labled PNPs for 0.5 or 2 h, respectively. Then the extracellular drug was washed with cold PBS for 3 times. Finally, the cells were collected, centrifuged, and resuspended with 0.3 ml of PBS. The intracellular fluorescence intensity was detected by using a FACS calibur flow cytometer.

2.10. Animal studies

All the animal experiments were approved by the Institutional Animal Ethical Care Committee (IAEC) of Shenyang Pharmaceutical University and conducted according to the Guidelines for the Care and Use of Laboratory Animals.

2.11. Pharmacokinetics

Healthy SD rats (180–220 g) were employed for pharmacokinetics studies. Briefly, DTX solution (5 mg/kg) or PNPs (DTX equivalent concentration: 5 mg/kg) were intravenously administrated. At presupposed timed intervals (0.083, 0.25, 0.5, 1, 2, 4, 8, 12 h), 400 μl of whole blood was taken and immediately centrifuged to acquire plasma. The plasma concentrations of prodrugs and released DTX were detected by UPLC-MS-MS with protein precipitation, using diazepam as the internal standard.

2.12. Biodistribution

4T1 breast tumor BALB/C mice xenograft model was established to evaluate biodistribution of PNPs. The mice were intravenously administrated with DiR solution (2 mg/kg) or DiR-labeled PNPs (DiR equivalent concentrations: 2 mg/kg) upon the tumor volume reached ~500 mm^3. Fluorescence imaging was obtained at 4, 8, 12 and 24 h after administration. At 24 h post administration, the mice were sacrificed for the observation of DiR accumulation in organs (heart, liver, spleen, lung and kidney) and tumors by applying small-animal living imaging system (IVIS spectrum).

2.13. In vivo antitumor efficacy

To evaluate *in vivo* antitumor activity of PNPs, the 4T1 breast cancer BALB/C mice xenograft model was established. Briefly, 4T1 cells were injected subcutaneously into the mice (5×10^6 cells/mice). And then the mice were divided into seven groups upon the tumor size was around 150 mm^3. Then, saline, DTX solution, SA-S-S-DTX NPs, EA-S-S-DTX NPs, OA-S-S-DTX NPs, LA-S-S-DTX NPs, LNA-S-S-DTX NPs were administrated intravenously to mice every second day (DTX equivalent dose: 10 mg/kg) for a total of five injections. Twelve days after first dose, plasma was collected for hepatic and renal function analysis, then the mice were sacrificed humanely and the major organs and tumors were fixed by 4% paraformaldehyde for hematoxylin and eosin (H&E) staining.

2.14. Statistical analysis

The data were displayed as mean values ± standard deviation (SD). Comparison of groups was judged using one-way ANOVA and student's *t*-test; difference was considered significant when $P < 0.05$.

3. Results and discussions

3.1. Synthesis of prodrugs

Five prodrugs (SA-S-S-DTX, EA-S-S-DTX, OA-S-S-DTX, LA-S-S-DTX, LNA-S-S-DTX) were successfully synthesized were characterized using MS and ^{1}H NMR (Fig. S1–S5).

3.2. Fabrication and characterization of PNPs

One-step nanoprecipitation method was utilized to fabricate PNPs [38]. Multiple interactions and forces participated in the self-assembly of these aliphatic prodrugs, mainly including: (i) the structural flexibility of aliphatic tails; (ii) the bond angle of disulfide bonds; (iii) intermolecular π-π stacking; and (iv) intermolecular hydrophobic interactions. To our surprise, only the EA-S-S-DTX prodrug with trans-FA could not assemble into NPs without the help of DSPE-$MPEG_{2000}$, but other prodrugs with cis-FAs could self-assembled into uniform and stable NPs with particle size about 100 nm (Fig. S6, Table S1). These results suggested that the cis-trans configuration of aliphatic tails imposed significant influence on the self-assembly characteristics of prodrugs. Obviously, cis-FAs seem to be more beneficial to the stable assembly of disulfide bond-linked aliphatic prodrugs. This could be a very interesting finding, probably due to the better steric flexibility of cis-FAs.

Our previous studies have demonstrated that non-PEGylated NPs showed very poor stability in PBS and short circulation time in blood because of their poor stability in salt solutions and blood [37]. Therefore, DSPE-$MPEG_{2000}$ was used to prepare PEGylated PNPs. As showed in Fig. S7 and Table S2, all these prodrugs could self-assemble into spherical NPs (70–80 nm) with negative surface charge (~30 mV) with the assistance of DSPE-$MPEG_{2000}$. Notably, these self-assemblied prodrug NPs had ultrahigh drug-loading capacity (>50%, w/w). More importantly, the utilization of Tween 80 and ethanol were completely avoided in these nano-formulations when compared with the commercially available injection of DTX (Taxotere®), significantly improving its biosafety and reducing excipient-associated side effects.

3.3. Chemical stability of prodrugs and colloidal stability of nanoassemblies

The initial purity of these prodrugs exceeded 98% after purification by preparative liquid chromatography. We then explored the storage chemical stability of the prodrugs at

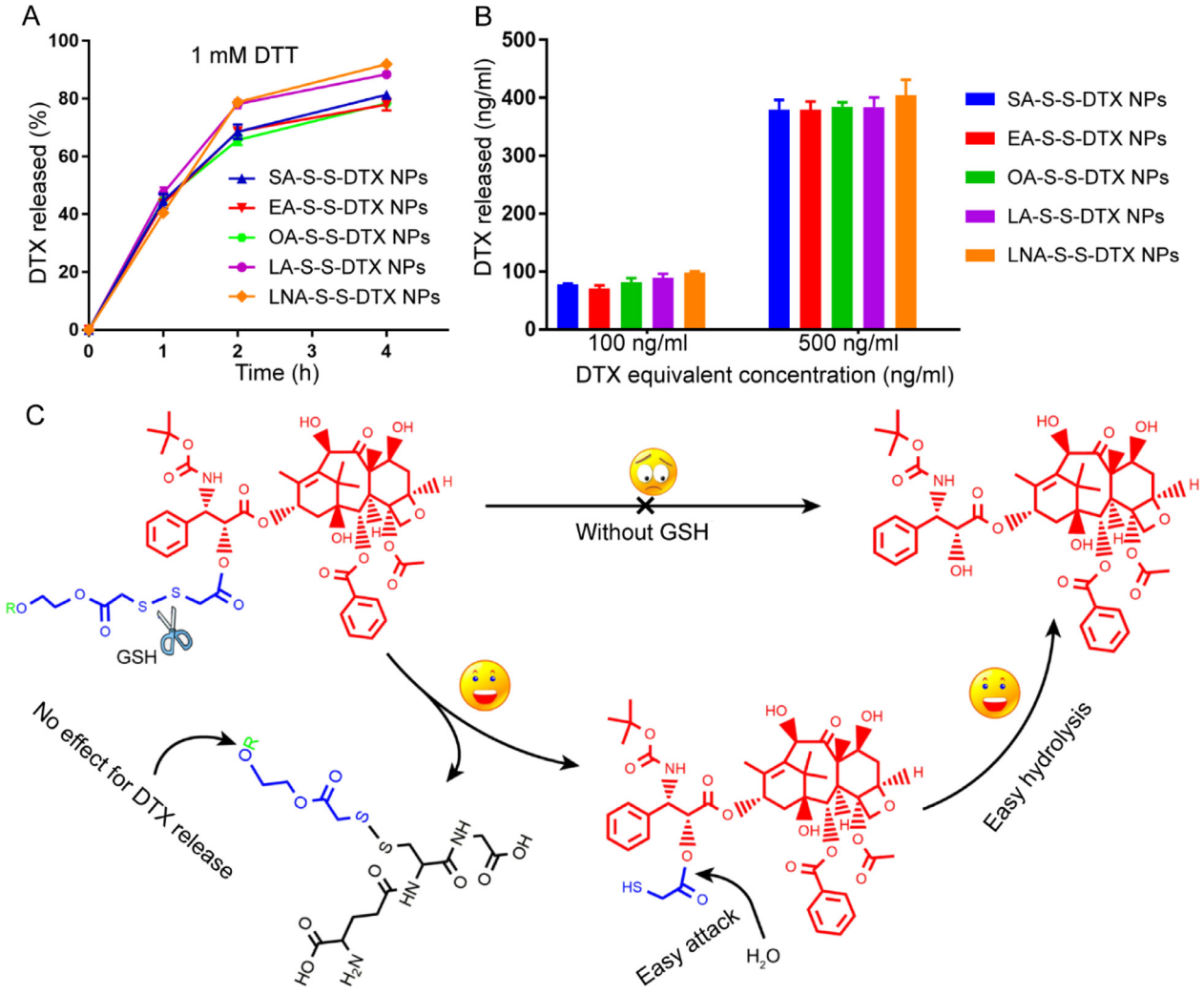

Fig. 1 – *In vitro* release of different FA-S-S-DTX. (A) The DTX release curve of different PNPs in PBS medium with 1 mM DTT. (B) Intracellular DTX release performance of different PNPs. (C) The release mechanisms of different FA-conjugated DTX prodrug via disulfide bond.

−20 °C using HPLC. As shown in Fig. S8, LA-S-S-DTX and LNA-S-S-DTX with two and three double bonds in the aliphatic chains showed poor chemical stability after storage at −20 °C. By contrast, the other three prodrugs without or with one double bond in the aliphatic chains kept good chemical stability. Therefore, the number of double bonds could exert significant impacts on the chemical stability of aliphatic prodrugs. More double bonds less stable.

Besides, the colloidal stability of these PNPs was also studied. As showed in Fig. S9, the particle size of non-PEGylated nanoassemblies of EA-S-S-DTX NPs, LA-S-S-DTX NPs and LNA-S-S-DTX NPs significantly increased, and obvious precipitates were observed in the tubes after storage at 4 °C for a week (Fig. S10). In contrast, the non-PEGylated nanoassemblies of SA-S-S-DTX and OA-S-S-DTX still kept good stability under the same conditions. Moreover, the long-term stability results of PEGylated PNPs suggested that the particle size of EA-S-S-DTX NPs, LA-S-S-DTX NPs and LNA-S-S-DTX NPs significantly increased (Fig. S11). By contrast, SA-S-S-DTX NPs and OA-S-S-DTX NPs exhibited good colloidal stability during the long-term stability test for two months. The poor stability of EA-S-S-DTX NPs should be attributed to the poor self-assembly ability of EA-S-S-DTX prodrug. On the other hand, the inferior chemical stability of LA-S-S-DTX and LNA-S-S-DTX led to the poor long-term stability of LA-S-S-DTX NPs and LNA-S-S-DTX NPs. These results further demonstrated that PEGylation modification really help the assembly process of aliphatic prodrugs, but the chemical and colloidal stability of PNPs could not be fundamentally changed. Moreover, the chemical stability of prodrugs is very important for self-assembled PNP. If the prodrugs were hydrolyzed, their self-assembly capacity significantly reduced. As a result, the non-covalent interactions between molecules could be weakened, leading to poor stability of NPs. Therefore, it's necessary to optimize the structure details of prodrugs for the future development of PNPs.

3.4. *Drug release from PNPs*

Drug release from prodrugs is extremely important for their anti-proliferative activity. Hence, the reduction-responsive

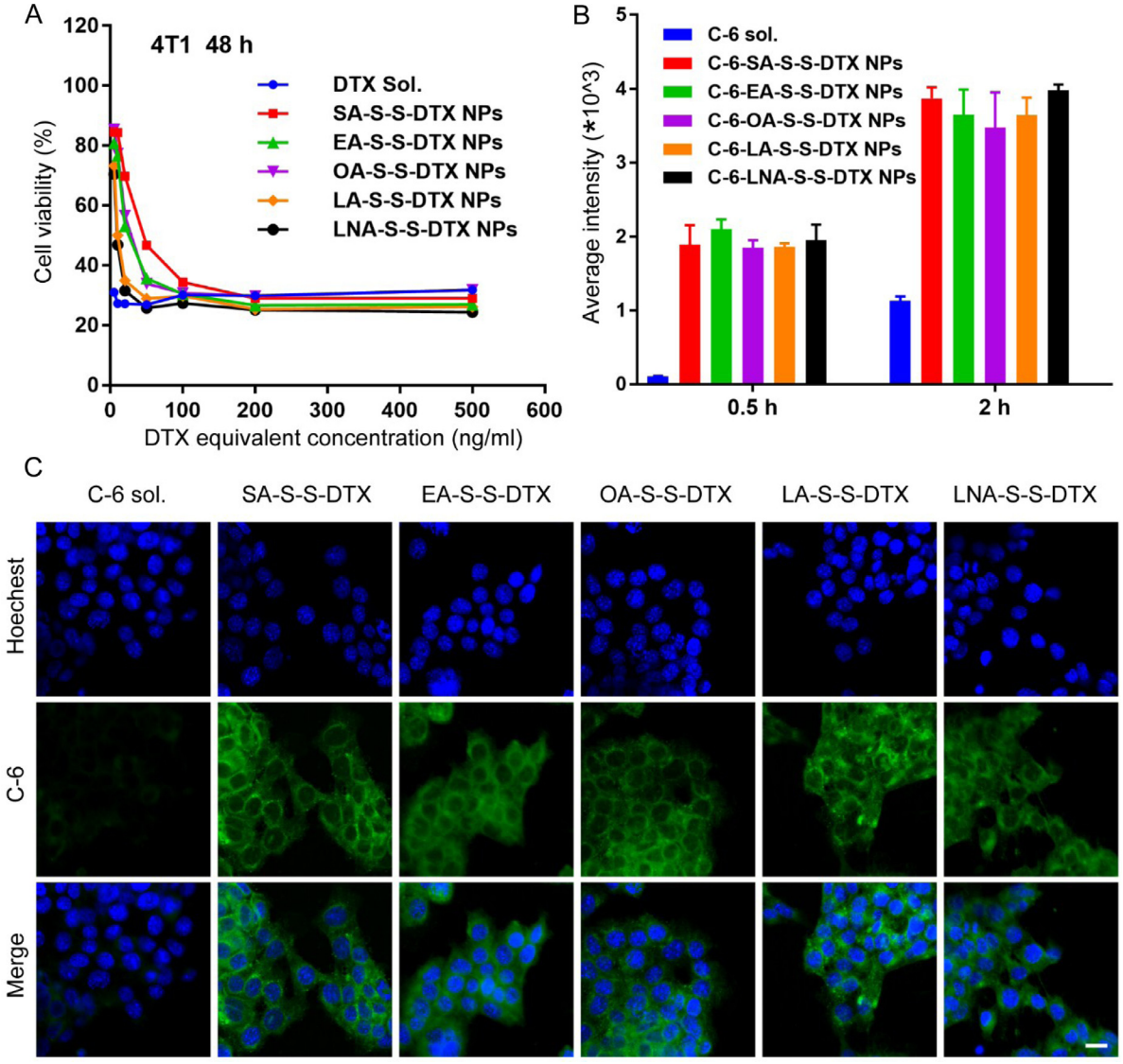

Fig. 2 – Cytotoxicity and cellular uptake of FA-S-S-DTX PNPs ($n = 3$). (A) Growth-inhibitory curves of 4T1 cells after treatment with DTX sol and FA-S-S-DTX PNPs for 48 h by MTT assays. (B) Cellular uptake in 4T1 cells incubated with free C-6 or C-6-labeled PNPs for 0.5 and 2 h evaluated by flow cytometry. (C) CLSM images of 4T1 cells incubated with C-6 sol or C-6-labeled PNPs for 2 h. Scale bar represents 10 μm.

drug release behavior of PNPs was investigated. PBS in the present of DTT (1 mM, a prevailing analogue of GSH) was utilized as *in vitro* release medium to mimic reductive tumor cellular microenvironment. As showed in Fig. 1A, almost all the DTX could be released from these PNPs within 4 h. Moreover, as shown in Fig. S12, almost all the DTX could also be quickly released from these PNPs within low concentrations of DTT (0.1 mM/0.5 mM), which demonstrated excellent reduction-responsiveness of prodrug nanoassemblies. Notably, there was almost no significant difference among these PNPs, due to the unique disulfide bond-mediated drug release mechanism (Fig. 1C). As shown in Fig. 1C, once the disulfide bond in the prodrugs was cracked by DTT, the FA segments were removed from the prodrugs, leaving the same intermediate with thiol group. Then, the thiol group facilitated the degradation of ester bond, resulting in rapid release of DTX. To further investigate the drug release behavior from prodrugs in the presence of intracellular redox stimuli, the DTX released from PNPs incubated with tumor cells was determinized using UPLC-MS-MS. Intracellular drug release amount showed a concentration-dependent way (Fig. 1B). But there's no significant difference among the different prodrugs, which was consistent with the release results in PBS medium containing DTT (Fig. 1A). These results suggested that different aliphatic tails accounted for almost no effect for reduction-responsive drug release from these PNPs, due to the specific drug release mechanism of disulfide bond-inserted prodrugs (Fig. 1C).

3.5. *In vitro anti-proliferative activity*

The anti-proliferative activity of DTX sol and PNPs against mouse breast carcinoma cells (4T1 cells), mouse hepatocellular carcinoma cells (Hepa 1-6 cells) and human normal hepatocytes (L02 cells) was evaluated by MTT assay.

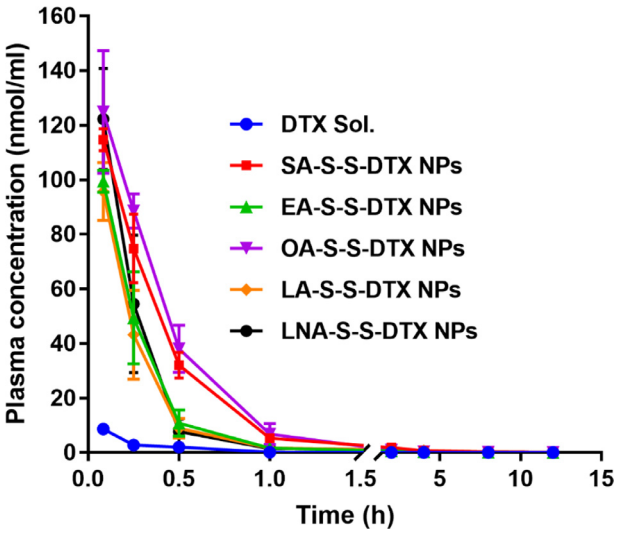

Fig. 3 – Total molar concentration-time curves of prodrugs and released DTX from prodrugs ($n = 5$).

The half maximal inhibitory concentrations (IC_{50} values) were shown in Table S3. As shown in Fig. 2A and Fig. S13A-S13D, PNPs showed comparable anti-proliferation ability when compared with DTX sol, further confirming the rapid DTX release from the PNPs in the within tumor cells. As expected, there was no significant difference among the different PNPs. That's because the *in vitro* cytotoxicity heavily depends on the drug release from prodrugs, and these PNPs showed no distinct difference in intracellular drug release (Fig. 1B). More importantly, PNPs exhibited lower cytotoxicity in normal cells (L02 cells) when compared with DTX sol, due to the slow DTX release from disulfide bond-bridged prodrugs in the comparatively low reductive microenvironment of normal cells (Fig. S13E-F), suggesting the excellent therapeutic selectivity of PNPs between tumor cells and normal cells.

3.6. *Cellular uptake*

Coumarin-6-labeled PNPs were prepared to investigate their cellular uptake efficiency. As shown in Fig. 2B-2C, the

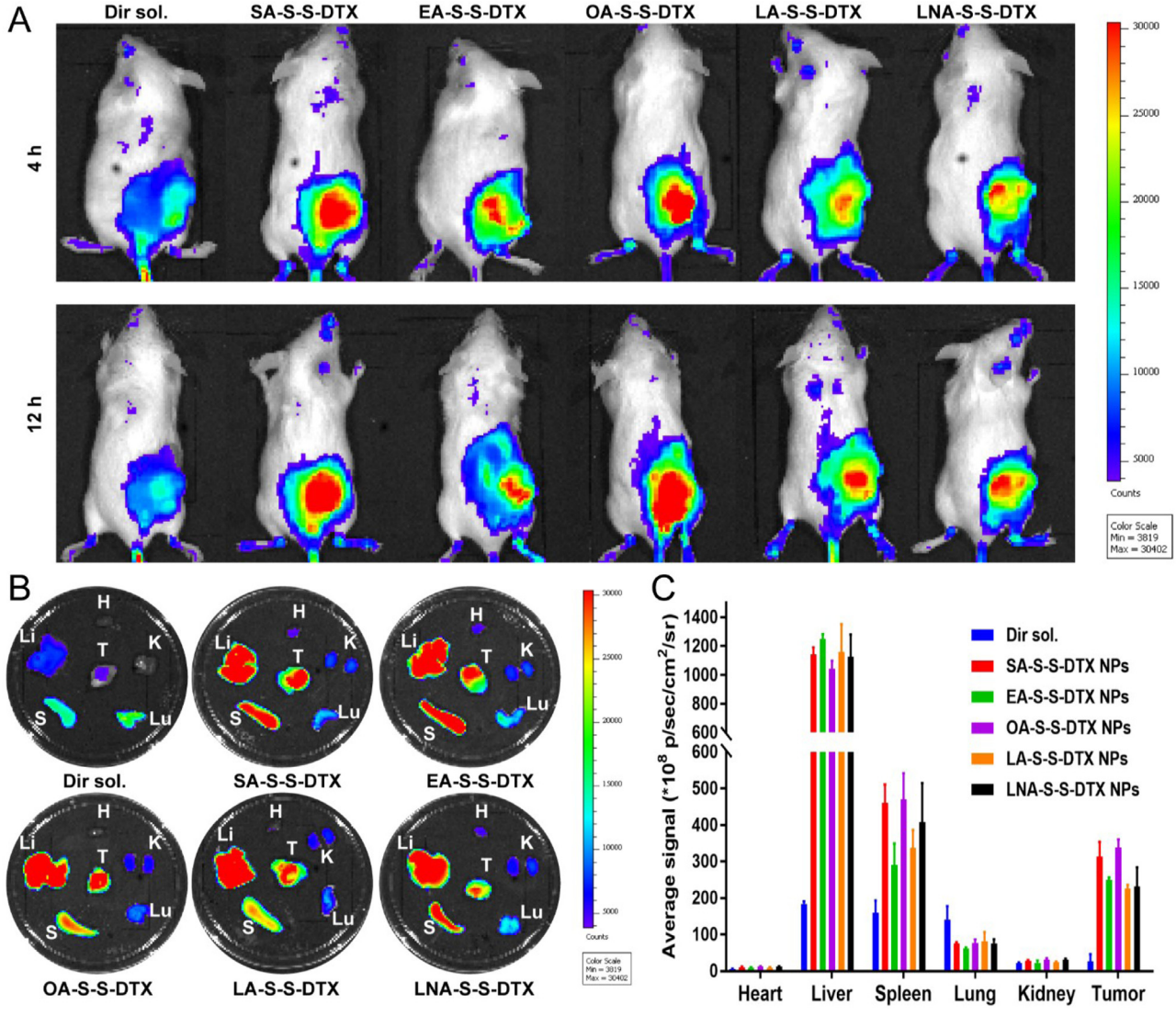

Fig. 4 – *In vivo* biodistribution of DiR sol and DiR-labeled PNPs. (A) *In vivo* fluorescent imaging at 4 or 12 h. (B) Fluorescent imaging of major organs and tumors at 24 h. (C) Quantitative determination of organ and tumor accumulation at 24 h. ($n = 3$).

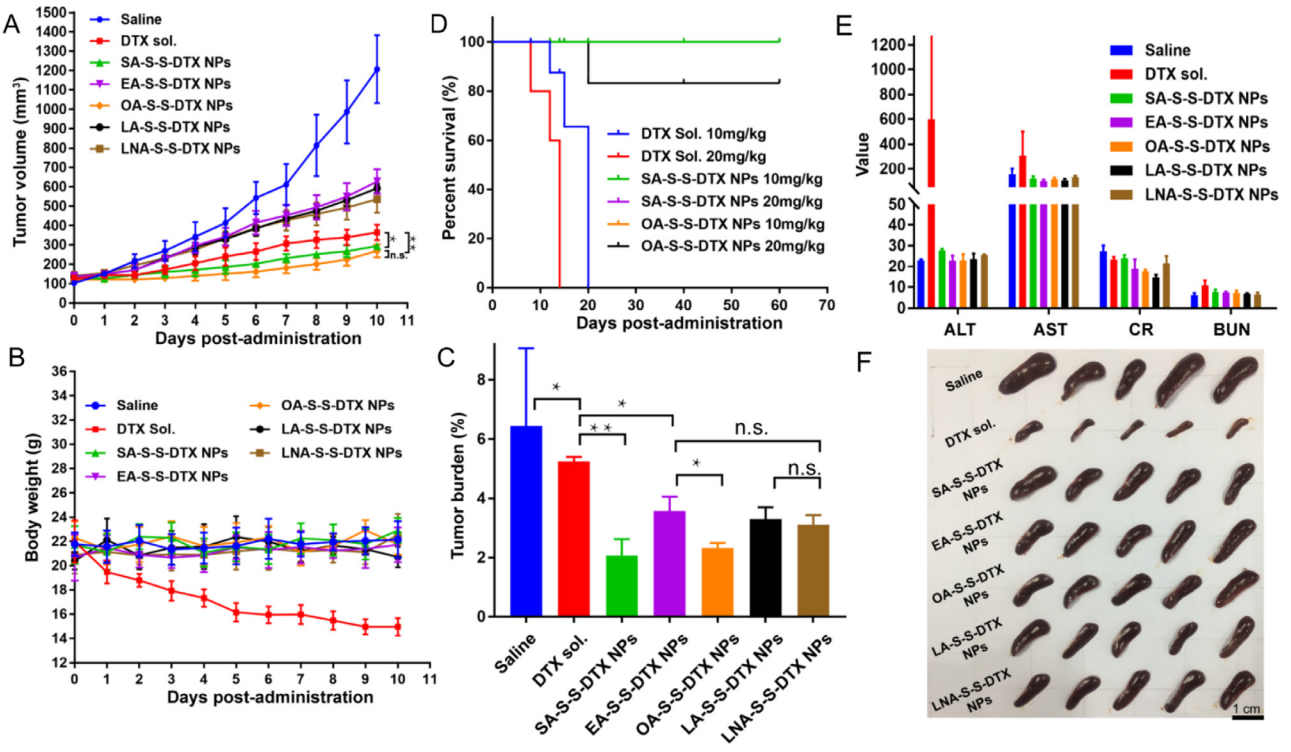

Fig. 5 – *In vivo* antitumor efficacy and safety evaluation of PNPs. (A) Tumor volume-time curve. (B) Mice body weight changes. (C) Tumor burden. (D) Survivorship curve of 4T1 tumor-bearing mice following intravenous injection of different doses of DTX sol, SA-S-S-DTX NPs, and OA-S-S-DTX NPs (at DTX-equivalent doses) ($n = 5$). (E) Hepatorenal function parameters ($n = 3$). Aspertate aminotransferase (AST, U/l); alanine aminotransferase (ALT, U/l); blood urea nitrogen (BUN, mmol/l); creatinine (CR, μmol/l). (f) Images of spleens after treatment.

cellular uptake of both coumarin-6 sol and coumarin-6-labled PNPs demonstrated a time-dependent way. Notably, the 4T1 cells incubated with coumarin-6-loaded PNPs presented exhibited stronger fluorescence signals than that incubated with coumarin-6 sol at both 0.5 and 2 h. These results demonstrated that PNPs had higher cellular uptake efficiency than free drugs. Moreover, there's no significant difference among these PNPs, due to their very similar nanostructure, particle size and morphology.

3.7. *Pharmacokinetics*

SD rats were utilized to explore the pharmacokinetic behaviors of DTX sol and PNPs. The concentrations of the prodrugs and the released DTX in plasma were determined using UPLC-MS/MS. The sum concentration-time curves were illustrated (Fig. 3), and the pharmacokinetic parameters were calculated in Table S4 by using DAS 2.0 software. As expected, all these PNPs exhibited prolonged circulation time in blood when compared with DTX sol (Fig. 3 and S14), owing to the protection effect of outer hydrophilic PEGylated layer on the surface. Notably, different aliphatic tails had evident impact on the pharmacokinetic behavior of PNPs. As shown in Fig. 3, SA-S-S-DTX NPs and OA-S-S-DTX NPs with good chemical stability and colloidal stability demonstrated distinct advantages over the other three nano-formulations. As previously discussed, EA-S-S-DTX demonstrated poor self-assembly capacity, resulting in poor colloidal stability (Fig. S9-S11), leading to quicker clearance from in blood when compared with SA-S-S-DTX NPs and OA-S-S-DTX NPs. In addition, the inferior pharmacokinetic profiles of LA-S-S-DTX NPs and LNA-S-S-DTX NPs should be attributed to both the poor chemical stability and colloidal stability of these two prodrugs (Fig. S8-S11). These results suggested that the undesirable properties of prodrugs exert crucial impacts on the *in vivo* drug delivery fate of PNPs.

3.8. *In vivo biodistribution*

To study the tumor accumulative capacity in 4T1 tumor-bearing mice, DiR was utilized to label the PNPs. As shown in Fig. 4, the mice received DiR-labeled PNPs exhibited significantly higher fluorescent intensity in tumors when compared with the mice treated with DiR sol at 4, 12 and 24 h, which should be contributed to prolonged circulation time in blood and the EPR effect-mediated passive targeting delivery of NPs. As expected, SA-S-S-DTX NPs/OA-S-S-DTX NPs exhibited higher fluorescent intensity in tumors than that of EA-S-S-DTX NPs, LA-S-S-DTX NPs and LNA-S-S-DTX NPs, which was consisted with the pharmacokinetics results (Fig. 3). These results suggested that different aliphatic tails significantly affected the tumor accumulation of PNPs by influencing the chemical stability, self-assembly ability, colloidal stability and circulation fate in blood of disulfide bond-bridged prodrugs.

3.9. *In vivo antitumor efficacy*

4T1 tumor-bearing mice were established to assess the *in vivo* antitumor efficacy of DTX sol and PNPs. As shown in Fig. 5, DTX sol, EA-S-S-DTX NPs, LA-S-S-DTX NPs and LNA-S-S-DTX NPs showed weaker antitumor effects when compared with SA-S-S-DTX NPs and OA-S-S-DTX NPs. The therapeutic advantages of SA-S-S-DTX NPs and OA-S-S-DTX NPs should be attributes to the following aspects: (i) good chemical stability; (ii) excellent self-assembly capacity and colloidal stability; (iii) high cellular uptake efficiency and rapid drug release in tumor cells; and (iv) their distinct advantages in systemic circulation and tumor accumulation. Notably, DTX sol still demonstrated more potent tumor-inhibiting efficacy than that of EA-S-S-DTX NPs, LA-S-S-DTX NPs and LNA-S-S-DTX NPs. The poor antitumor activity of EA-S-S-DTX NPs, LA-S-S-DTX NPs and LNA-S-S-DTX NPs should be attributed to their poor chemical and colloidal stability, as well as the delayed drug release from prodrugs within tumors. By contrast, there's no drug release process for DTX sol, and the tumor cells were directly exposed to DTX. As shown in Table S3, DTX sol had a lower IC_{50} value than that of EA-S-S-DTX NPs, LA-S-S-DTX NPs and LNA-S-S-DTX NPs.

Then, the systemic toxicity of DTX sol and PNPs was investigated. As shown in Fig. 5B, the mice body weight significantly reduced along with the treatment of DTX sol, suggesting severe systemic toxicity. By contrast, there's no significant body change observed in the group treated with PNPs. Additionally, the hepatorenal function parameters were examined after the final treatment (Fig. 5E). The abnormal AST and ALT values indicated potential hepatotoxicity caused by DTX sol. Moreover, the dramatically atrophic spleens in the DTX sol group also indicated the organ systemic toxicity of DTX sol. In order to further assess the good safety of the PNPs, higher doses of DTX sol (10/20 mg/kg) and PNPs (10/20 mg/kg, equivalent dose of DTX) were administered intravenously to the 4T1 breast tumor-bearing BALB/C mice. The mice received DTX sol died quickly both in 10/20 mg/kg dose, but the mice treated with PNPs showed good survival even at 20 mg/kg dose (Fig. 5D). All these results indicated that the PNPs not only significantly improved the anti-tumor efficacy, but greatly reduced the systemic toxicity of DTX.

4. Conclusions

To sum up, the present study focused on the possible influence of different aliphatic moieties on disulfide bond-bridged lipophilic PNPs. Five prodrugs of DTX were designed and synthesized by using different FAs with different saturation and cis-trans configuration as aliphatic tails. Most of these aliphatic prodrugs readily assemble into PNPs with ultra-high drug loading rate (>55%, w/w). The effects of the saturation and cis-trans configuration of aliphatic tails on the assembly features, stability and drug delivery fate of PNPs were investigated in detail. This is the first study to show that the cis-trans configuration of aliphatic tails significantly influences the self-assembly process of disulfide bond-bridged lipophilic prodrugs. It turned out that EA-S-S-DTX with a trans double bond in the aliphatic chain showed poor self-assembly capacity. Although the aliphatic tails have almost no effect on the redox-sensitive drug release and cytotoxicity, different aliphatic tails significantly influence the chemical stability of prodrugs and the colloidal stability of PNPs, thus significantly affecting their *in vivo* pharmacokinetics, biodistribution and antitumor efficacy. Our studies offer new insight into the side chain details of disulfide bond-bridged prodrugs, and provided knowledges for rational design of PNPs for efficient anticancer drug delivery.

Conflicts of interest

The authors report no conflicts of interest.

Acknowledgments

The authors acknowledge funding from the National Natural Science Foundation of China (No. 81703451 and 81773656), the Excellent Youth Science Foundation of Liaoning Province (No. 2020-YQ-06), the Liaoning Revitalization Talents Program (No. XLYC1808017 and XLYC1907129), the China Postdoctoral Science Foundation (No. 2020M670794), and the Science and Technology Major Project of Liaoning (No. 2019JH1/10300004). The authors acknowledge Suzhou Yutai Pharmaceutical Technology Co. LTD for prodrugs synthesis process and some samples.

Supplementary materials

Supplementary material associated with this article can be found, in the online version, at doi:10.1016/j.ajps.2021.02.001.

REFERENCES

[1] Siegel RL, Miller KD, Jemal A. Cancer statistics, 2020. CA Cancer J Clin 2020;70:7–30.
[2] He H, Liu L, Morin EE, Liu M, Schwendeman A. Survey of clinical translation of cancer nanomedicines—Lessons learned from successes and failures. Acc Chem Res 2019;52:2445–61.
[3] Chen Q, Liu G, Liu S, Su H, Wang Y, Li J, et al. Remodeling the tumor microenvironment with emerging nanotherapeutics. Trends Pharmacol Sci 2018;39:59–74.
[4] Shan X, Li S, Sun B, Chen Q, Sun J, He Z, et al. Ferroptosis-driven nanotherapeutics for cancer treatment. J Control Rel 2020;319:322–32.
[5] Zhang E, Xing R, Liu S, Li P. Current advances in development of new docetaxel formulations. Expert Opin Drug Deliv 2019;16:301–12.
[6] Li S, Shan X, Wang Y, Chen Q, Sun J, He Z, et al. Proceedings of the national academy of sciences asian journal of pharmaceutical sciencesdimeric prodrug-based nanomedicines for cancer therapy. J Control Rel 2020;326:510–22.
[7] Zhang S, Guan J, Sun M, Zhang D, Zhang H, Sun B, et al. Self-delivering prodrug-nanoassemblies fabricated by

disulfide bond bridged oleate prodrug of docetaxel for breast cancer therapy. Drug Deliv 2017;24:1460–9.
[8] Zhou S, Shang Q, Wang N, Li Q, Song A, Luan Y. Rational design of a minimalist nanoplatform to maximize immunotherapeutic efficacy: four birds with one stone. J Control Rel 2020;328:617–30.
[9] Li A, Zhao J, Fu J, Cai J, Zhang P. Recent advances of biomimetic nano-systems in the diagnosis and treatment of tumor. Asian J Pharm Sci 2019.
[10] Sun Q, Zhou Z, Qiu N, Shen Y. Rational design of cancer nanomedicine: nanoproperty integration and synchronization. Adv Mater 2017;29:1606628.
[11] Golombek SK, May J, Theek B, Appold L, Drude N, Kiessling F, et al. Tumor targeting via epr: strategies to enhance patient responses. Adv Drug Deliv Rev 2018;130:17–38.
[12] Maeda H. Toward a full understanding of the epr effect in primary and metastatic tumors as well as issues related to its heterogeneity. Adv Drug Deliv Rev 2015;91:3–6.
[13] Mu W, Chu Q, Liu Y, Zhang N. A review on nano-based drug delivery system for cancer chemoimmunotherapy. Nanomicro Lett 2020;12:142.
[14] Zhang H, Zhang J, Li Q, Song A, Tian H, Wang J, et al. Site-specific mof-based immunotherapeutic nanoplatforms via synergistic tumor cells-targeted treatment and dendritic cells-targeted immunomodulation. Biomaterials 2020;245:119983.
[15] Tian H, Zhang M, Jin G, Jiang Y, Luan Y. Cu-mof chemodynamic nanoplatform via modulating glutathione and h2o2 in tumor microenvironment for amplified cancer therapy. J Colloid Interface Sci 2020;587:358–66.
[16] Zhou Y, Ren X, Hou Z, Wang N, Jiang Y, Luan Y. Engineering a photosensitizer nanoplatform for amplified photodynamic immunotherapy via tumor microenvironment modulation. Nanoscale Horiz 2021;6:120–31.
[17] Wolfram J, Ferrari MJNT. Clinical cancer nanomedicine. Nano Today 2019;25:85–98.
[18] Shi J, Kantoff PW, Wooster R, Farokhzad OC. Cancer nanomedicine: progress, challenges and opportunities. Nat Rev Cancer 2017;17:20–37.
[19] Zhang X, Li N, Zhang S, Sun B, Chen Q, He Z, et al. Emerging carrier-free nanosystems based on molecular self-assembly of pure drugs for cancer therapy. Med Res Rev 2020;40:1754–75.
[20] Zhang X, Sun B, Zuo S, Chen Q, Gao Y, Zhao H, et al. Self-assembly of a pure photosensitizer as a versatile theragnostic nanoplatform for imaging-guided antitumor photothermal therapy. ACS Appl Mater Interfaces 2018;10:30155–62.
[21] Li Y, Lin J, Wang P, Luo Q, Zhu F, Zhang Y, et al. Tumor microenvironment cascade-responsive nanodrug with self-targeting activation and ros regeneration for synergistic oxidation-chemotherapy. Nanomicro Lett 2020;12:182.
[22] Luo C, Sun J, Sun B, Liu D, Miao L, Goodwin TJ, et al. Facile fabrication of tumor redox-sensitive nanoassemblies of small-molecule oleate prodrug as potent chemotherapeutic nanomedicine. Small 2016;12:6353–62.
[23] Harries M, O'donnell A, Scurr M, Reade S, Cole C, Judson I, et al. Phase i/ii study of dha-paclitaxel in combination with carboplatin in patients with advanced malignant solid tumours. Br J Cancer 2004;91:1651–5.
[24] Zeng J, Li C, Duan X, Liu F, Li A, Luo C, et al. Pegylation of lipophilic sn38 prodrug with dspe-mpeg2000 *versus* cremophor el: comparative study for intravenous chemotherapy. Drug Deliv 2019;26:354–62.
[25] Mura S, Nicolas J, Couvreur P. Stimuli-responsive nanocarriers for drug delivery. Nat Mater 2013;12:991–1003.
[26] Van Der Meel R, Sulheim E, Shi Y, Kiessling F, Mulder WJM, Lammers T. Smart cancer nanomedicine. Nat Nanotechnol 2019;14:1007–17.
[27] Yang N, Xiao W, Song X, Wang W, Dong X. Recent advances in tumor microenvironment hydrogen peroxide-responsive materials for cancer photodynamic therapy. Nanomicro Lett 2020;12:15.
[28] Wang J, Sun X, Mao W, Sun W, Tang J, Sui M, et al. Tumor redox heterogeneity-responsive prodrug nanocapsules for cancer chemotherapy. Adv Mater 2013;25:3670–6.
[29] Yang B, Wei L, Wang Y, Li N, Ji B, Wang K, et al. Oxidation-strengthened disulfide-bridged prodrug nanoplatforms with cascade facilitated drug release for synergetic photochemotherapy. Asian J Pharm Sci 2020;15:637–45.
[30] Sun B, Luo C, Zhang X, Guo M, Sun M, Yu H, et al. Probing the impact of sulfur/selenium/carbon linkages on prodrug nanoassemblies for cancer therapy. Nat Commun 2019;10:3211.
[31] Wang K, Yang B, Ye H, Zhang X, Song H, Wang X, et al. Self-strengthened oxidation-responsive bioactivating prodrug nanosystem with sequential and synergistically facilitated drug release for treatment of breast cancer. ACS Appl Mater Interfaces 2019;11:18914–22.
[32] Sun B, Chen Y, Yu H, Wang C, Zhang X, Zhao H, et al. Photodynamic peg-coated ros-sensitive prodrug nanoassemblies for core-shell synergistic chemo-photodynamic therapy. Acta Biomater 2019;92:219–28.
[33] Wang Y, Liu D, Zheng Q, Zhao Q, Zhang H, Ma Y, et al. Disulfide bond bridge insertion turns hydrophobic anticancer prodrugs into self-assembled nanomedicines. Nano Lett 2014;14:5577–83.
[34] Yang Y, Sun B, Zuo S, Li X, Zhou S, Li L, et al. Trisulfide bond–mediated doxorubicin dimeric prodrug nanoassemblies with high drug loading, high self-assembly stability, and high tumor selectivity. Sci Adv 2020;6:eabc1725.
[35] Yang F, Zhao Z, Sun B, Chen Q, Sun J, He Z, et al. Nanotherapeutics for antimetastatic treatment. Trends Cancer 2020;6:645–59.
[36] Li M, Zhao L, Zhang T, Shu Y, He Z, Ma Y, et al. Redox-sensitive prodrug nanoassemblies based on linoleic acid-modified docetaxel to resist breast cancers. Acta Pharm Sin B 2019;9:421–32.
[37] Luo C, Sun J, Liu D, Sun B, Miao L, Musetti S, et al. Self-assembled redox dual-responsive prodrug-nanosystem formed by single thioether-bridged paclitaxel-fatty acid conjugate for cancer chemotherapy. Nano Lett 2016;16:5401–8.
[38] Sun B, Luo C, Yu H, Zhang X, Chen Q, Yang W, et al. Disulfide bond-driven oxidation- and reduction-responsive prodrug nanoassemblies for cancer therapy. Nano Lett 2018;18:3643–50.